

RSC Advances



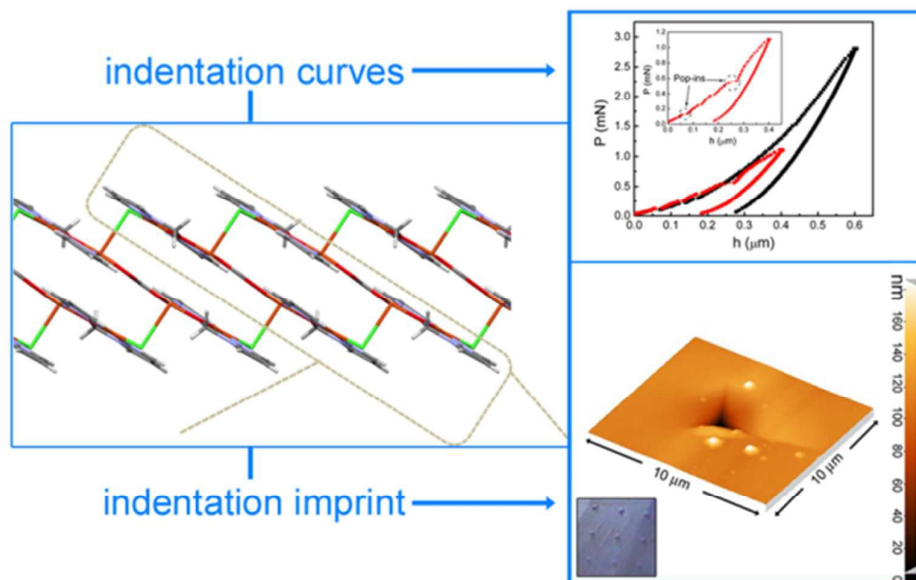
This is an *Accepted Manuscript*, which has been through the Royal Society of Chemistry peer review process and has been accepted for publication.

Accepted Manuscripts are published online shortly after acceptance, before technical editing, formatting and proof reading. Using this free service, authors can make their results available to the community, in citable form, before we publish the edited article. This *Accepted Manuscript* will be replaced by the edited, formatted and paginated article as soon as this is available.

You can find more information about *Accepted Manuscripts* in the [Information for Authors](#).

Please note that technical editing may introduce minor changes to the text and/or graphics, which may alter content. The journal's standard [Terms & Conditions](#) and the [Ethical guidelines](#) still apply. In no event shall the Royal Society of Chemistry be held responsible for any errors or omissions in this *Accepted Manuscript* or any consequences arising from the use of any information it contains.

Graphical Abstract



Cite this: DOI: 10.1039/c0xx00000x

www.rsc.org/xxxxxx

COMMUNICATION

New binuclear Copper(II) Coordination Polymer based on Mixed Pyrazolic and Oxalate Ligands: Structural Characterization and Mechanical Properties

Adaris M. López-Marzo,^{a,†} Miguel Guerrero,^{b,†,*} Teresa Calvet,^c Mercè Font-Bardia,^d Eva Pellicer,^b Maria Dolors Baró,^b Josefina Pons,^{a,*} and Jordi Sort^c

Received (in XXX, XXX) Xth XXXXXXXXXX 20XX, Accepted Xth XXXXXXXXXX 20XX

DOI: 10.1039/b000000x

A new inorganic-organic coordination polymer based on copper(II) binuclear complex coordinated with pyrazole (**L1**), 1-(hydroxymethyl)pyrazole (**L2**) and oxalate (**Ox**) ligands has been unexpectedly obtained. The crystal structure of this coordination polymer has been unequivocally determined by single crystal X-ray diffraction. One copper(II) center (Cu1) is four coordinated with two nitrogens (N2, L1 and N3, L2), one oxygen (O1, L1) and one chlorine atoms, while the other copper(II) nucleus (Cu2) is five-coordinated with one nitrogen (N1, L1), three oxygen (O1, L2; O2 and O3, Ox) and one chlorine atoms giving slightly distorted square-planar and square-pyramidal geometries, respectively. To the best of our knowledge, such coordination environments have never been previously observed to coexist in the same structure. The terminal chlorine (Cl1) constitutes the connecting bridge between the planar binuclear [Cu₂Cl(Ox)_{0.5}(L1)(L2)]_n units ending in an attractive structural framework. An extending layered structure staggered along the *b*-axis is observed in the supramolecular view. Nanoindentation experiments were carried out and relevant mechanical parameters such as hardness, Young's modulus, indentation energies and elastic recovery have been determined. Additionally, a comparative analysis between the supramolecular structure and the mechanical properties is reported.

1. Introduction

The design of hybrid metal-organic materials (MOMs), which is a burgeoning topic in crystal engineering domain, is nowadays one of the fastest growing areas in the fields of Materials Science and Supramolecular Chemistry.^{1,2} This new class of materials attracts significant attention due to their enormous chemical, structural and topological diversity and due to their promising applications including catalysis, gas storage, magnetism, luminescence, drug delivery, sensing or host/guest inclusion.³⁻⁶ Interestingly, such hybrids systems present strong covalent and/or intermolecular bonds to yield 1D chains, 2D layers or 3D frameworks which incorporate at the same time 3d-metal ions and bridging ligands. The synergy between the organic and inorganic components brings about an outstanding combination of properties that are not common in purely inorganic and organic systems alone. Furthermore, the use of different ligands as building blocks with similar coordination ability but different flexibility could be considered as a smart procedure to obtain periodic frameworks.⁷⁻⁹

In contrast to the large number of recent publications describing the synthesis, and characterization of MOMs structures, studies focusing on understanding the mechanical properties of these hybrid materials are still scarce due to the lack of a proper measurement tools.¹⁰ Nonetheless, recent advances in this field are shedding some light on the fundamental structure-mechanical property relationships, which are needed for optimized design and successful performance in diverse technological applications.¹¹ Nanoindentation has emerged as a widely adopted technique for measuring the mechanical properties of different kinds of materials, such as ceramics, organics, inorganics and MOMs at nanoscale level.¹² This technique, where load (*P*) and penetration

depth (*h*) are measured with a high resolution, enables not only the evaluation of the mechanical properties but also the correlation between the measured responses and the underlying structural features and intermolecular interactions.¹³ This makes nanoindentation a complementary technique to structural analysis for the development of novel smart materials. In general, MOMs have been reported to be mechanically harder than inorganic polymers, while often exhibiting lower density values, similar to those of metallic foams.¹⁴

In this paper we present for the first time an inorganic-organic polymeric complex containing two different copper(II) cores with mixed oxalate ion and pyrazolic ligands. This new coordination polymer presents along the *b*-axis a 2D network formed by layers of stepped chains interconnected by bridge chlorine atoms (Cl1) through the Cu(1)-Cl(1)-Cu(2) bond. Hardness, Young's modulus, indentation energies and elastic recovery of this Cu(II) supramolecular inorganic/organic framework have been investigated by means of nanoindentation technique and compared with similar examples from the literature.

2. Experimental part

2.1 Reagents and Synthesis

All reagents were purchased from Sigma-Aldrich and used as received without further purification. 1-(hydroxymethyl)pyrazole (**L2**) was synthesized as described previously.¹⁵

In order to obtain the copper(II) based coordination complex, pyrazole (**L1**) and **L2** ligands were mixed with CuCl₂·2H₂O (1:1:2 molar ratio) during 18 h using ethanol as solvent under aerobic conditions. The pH was adjusted to 9 with ammonium hydroxide solution (30% NH₃). The green powder obtained as

product was washed by vacuum filtration with few milliliters of cold diethyl ether and dried at room temperature. Minority and translucent blue prism-like monocrystals suitable for X-ray analysis were obtained through the crystallization of the synthesis product by ethanol/dichloromethane (1:1) diffusion technique.

2.2 Characterization techniques

For X-ray crystallographic analysis a translucent blue prism-like specimen of $C_8H_8ClCu_2N_4O_3$ ($M_w=370.71 \text{ g mol}^{-1}$), $0.145 \text{ mm} \times 0.252 \text{ mm} \times 0.290 \text{ mm}$, was used. X-ray intensity data were measured on a D8 Venture system equipped with a multilayer monochromator and a Mo microfocus ($\lambda = 0.71073 \text{ \AA}$). A total of 682 frames were collected. The total exposure time was 1.89 hours. The frames were integrated with the Bruker SAINT Software package using a narrow-frame algorithm. The integration of the data using a monoclinic unit cell yielded a total of 13166 reflections to a maximum θ angle of 26.37° (0.80 \AA resolution), out of which 2283 were independent (average redundancy 5767, completeness = 99.8%, $R_{\text{int}} = 3.44\%$, $R_{\text{sig}} = 2.24\%$) and 2121 (92.90%) were greater than $2\sigma(F^2)$. Elemental analysis (C, H, N) of the monocrystal-like specimen was carried out on a Carlo Erba CHNS EA-1108 instrument separated by chromatographic column and thermoconductivity detector. Copper elemental analysis was carried out by using inductively coupled plasma mass spectrometry (ICPMS) Agilent 7500ce model system. Infrared Spectroscopy (IR) spectra were recorded on a Perkin-Elmer FT spectrophotometer series 2000 cm^{-1} as KBr pellets. Conductivity measurements were performed at room temperature in 10^{-3} M methanol solutions, employing a CyberScan CON 500 (Eutech instrument) conductimeter. Electronic spectra were run on a Kontron-Uvikon 860 in methanol between 750 and 350 nm.

2.3 Mechanical Properties

The mechanical properties (hardness, reduced elastic modulus and elastic recovery) were evaluated by means of nanoindentation, using an UMIS device from Fischer-Cripps Laboratories equipped with a Berkovich pyramidal-shaped diamond tip, operating in the load control mode. The nanoindentation tests were performed perpendicular to the planar base (100) of the crystal sheet. Other orientations were not possible due to the to the crystal exfoliation of the material. Indentations using maximum applied load values ranging from 1 to 5 mN were applied to ensure that the maximum penetration depth is much smaller than the crystal thickness. The indentations were separated from each other by $20 \mu\text{m}$, to ensure that the stress fields underneath the indents do not overlap with each other. The thermal drift during nanoindentation was lower than 0.05 nm s^{-1} . Proper corrections for the contact area (calibrated with a fused quartz specimen), instrument compliance, and initial penetration depth (a pre-contact load of 0.02 mN was used) were applied. The hardness (H) and reduced elastic modulus (E_r) values were derived from the load-displacement curves using the method of Oliver and Pharr.¹⁶ From the initial unloading slope, the contact stiffness, S , was determined as:

$$S = \frac{dP}{dh} \quad (1)$$

The reduced Young's modulus was evaluated based on its relationship with the contact area, A , and S :

$$S = \beta \frac{2}{\sqrt{\pi}} E_r \sqrt{A} \quad (2)$$

where β is the King's factor, that depends on the geometry of the indenter ($\beta = 1.034$ for a Berkovich indenter).¹⁷ The reduced Young's modulus takes into account the elastic displacements that occur in both the specimen, with Young's modulus E and Poisson's ratio ν , and the diamond indenter, with elastic constants E_i and ν_i (for diamond, $E_i = 1140 \text{ GPa}$ and $\nu_i = 0.07$):

$$\frac{1}{E_r} = \frac{1-\nu^2}{E} + \frac{1-\nu_i^2}{E_i} \quad (3)$$

The hardness was calculated from the following expression:

$$H = \frac{P_{\text{Max}}}{A} \quad (4)$$

where P_{Max} is the maximum load applied during nanoindentation. Finally, the elastic recovery was evaluated as the ratio between the elastic and the total (plastic + elastic) energies during nanoindentation, W_{el}/W_{tot} . The values of W_{el} were calculated as the area between the unloading curve and the displacement axis. In turn, W_{tot} is the area between the loading curve and the displacement axis.¹⁸ The results presented in this work are the statistical average of a set of 10 indentations at the applied maximum load.

3. Results and Discussion

3.1 Crystal structure of the binuclear copper(II) based coordination polymer

Reaction of L1 and L2 ligands with $\text{CuCl}_2 \cdot 2\text{H}_2\text{O}$ (1:1:2 molar ratio) was carried out in ethanol. The recrystallization of the reaction product afforded minority blue prism-like monocrystals. The X-ray diffraction measurements performed on the so-obtained monocrystals revealed that the complex crystallizes in the $P2(1)/c$ space group with two independent Cu(II) metal centers having square-planar and square-pyramidal geometries, respectively (Figure 1). The complex presents a polymeric structure showing a one-dimensional (1D) infinite neutral chain of planar binuclear $[\text{Cu}_2\text{Cl}(\text{Ox})_{0.5}(\text{L1})(\text{L2})]_n$ units wherein both L1-L2 ligands bridges adjacent the different copper(II) centers. Additional characterizations on these monocrystals were carried out.¹⁹

The local coordination environment around the four-coordinated Cu(II) atom (Cu1) is formed by two pyrazolyl (pz) nitrogen atoms (N2 and N3 in L1 and L2 ligands, respectively), one alcohol oxygen atom (O1, L2) and one bridged chlorine atom (Cl1). The coordination sphere of Cu1 can be described as a slightly distorted square-planar geometry with N2-Cu1-O1 and N3-Cu1-Cl1 angles between $81.17(7)^\circ$ and $94.26(5)^\circ$, respectively, which is within the expected range for copper(II) compounds with a square-planar geometry. The Cu1-O1, Cu1-N2 and Cu1-N3 bonds distances have similar values in the $1.937\text{-}1.945 \text{ \AA}$ range, indicating a stronger coordination than the Cu1-Cl1 bond (2.25 \AA). The $[\text{CuClO}(\text{N}_{\text{pz}})_2]$ core has been previously reported in the literature²⁰⁻²³ but never as a building block of a polymeric structure. Selected values of bond lengths and bond angles for the complex as well as the corresponding crystallographic data are shown in table 1 and table 2, respectively.

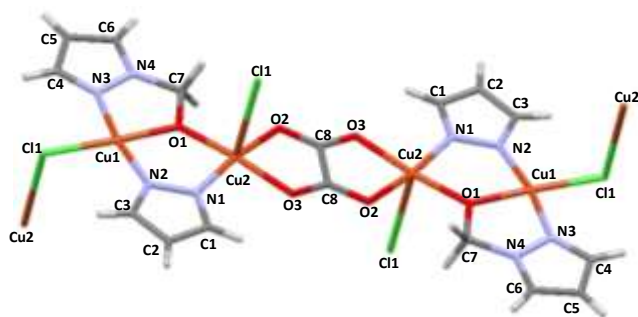


Figure 1. X-Ray structure of the $[\text{Cu}_4\text{Cl}_2(\text{Ox})(\text{L1})_2(\text{L2})_2]$ complex where the $[\text{Cu}_2\text{Cl}(\text{Ox})_{0.5}(\text{L1})(\text{L2})]$ is the basic monomeric unit of this polymeric chain. Scheme colour: copper, orange; oxygen, red; chlorine, green; nitrogen, blue and carbon, grey.

Table 1. Selected bond lengths (Å) and bond angles (°) values for a) square-planar and b) square-pyramidal copper(II) geometries of the complex. Symmetry code: #1 -x+1,-y+1,-z.

Geometries	bond lengths (Å) and bond angles (°)	
a)	Cu (1) – N (2)	1.9371(17)
	Cu (1) – N (3)	1.9441(18)
	Cu (1) – O (1)	1.9448(14)
	Cu (1) – Cl (1)	2.2569(5)
	N (2) – Cu (1) – O (1)	89.18(7)
	N (3) – Cu (1) – O (1)	81.17(7)
	N (2) – Cu (1) – Cl (1)	95.45(5)
N (3) – Cu (1) – Cl (1)	94.26(5)	
b)	Cu (2) – N (1)	1.9257(17)
	Cu (2) – O (1)	1.9318(14)
	Cu (2) – O (2)	1.9679(14)
	Cu (2) – O (3)#1	1.9991(14)
	Cu (2) – Cl (1)	2.795(4)
	N (1) – Cu (2) – O (1)	89.00(7)
	O (2) – Cu (2) – O (1)	95.59(6)
	N (1) – Cu (2) – O (3)#1	89.92(7)
	O (2) – Cu (2) – O (3)#1	84.78(6)
	O (3)#1 – Cu (2) – Cl (1)	92.57(5)

Regarding the five-coordinated Cu2 atom, the basal plane is formed by one pyrazolyl nitrogen atom (N1, L1), one alcohol oxygen atom (O1, L2) and two chelated oxygen atoms from oxalate anion (O2 and O3, Ox). These four coordinated atoms together with the Cu2 ion define almost perfect planar arrangement. The Cu2 atom is slightly displaced 0.124(2) Å from the apical position of the Cu2 site with a longer bond distance of 2.795(3) Å. The coordination sphere of Cu2 can be described as a slightly distorted square-pyramidal geometry with O(2)–Cu(2)–O(1) and O(2)–Cu(2)–O(3) angles between 84.78(6) and 95.59(6)°, respectively, and Cu(2)–O(1), Cu(2)–O(2), Cu(2)–O(3) and Cu(2)–N(1) bond distances with values of 1.932, 1.968, 1.999 and 1.926 Å, respectively. Such values of angles and bond distances are within the expected range for copper(II) compounds with square-pyramidal geometry. In the crystal structure the Cu2 metal centers with square-pyramidal geometry are connected to each other by one oxalate anion (Ox) ligand through a bis-bidentate chelating mode, with adjacent Cu(II) atoms at 5.164 Å (μ -oxalato- $1\text{k}^2\text{O}^1, \text{O}^2:2\text{k}\text{O}^1\text{a}, \text{O}^2\text{a}$). The Cu–Ox distances fall within the typical range for oxalate bridged Cu(II) complexes.^{24–26} The Cu1...Cu2 distance of 3.350 Å is out of the limit of interactive range between the different copper atoms (van der Waals radius of Cu(II) is 2.8 Å). The pyrazole rings are nearly parallel being the dihedral angle between their planes of 3.15(1)°.

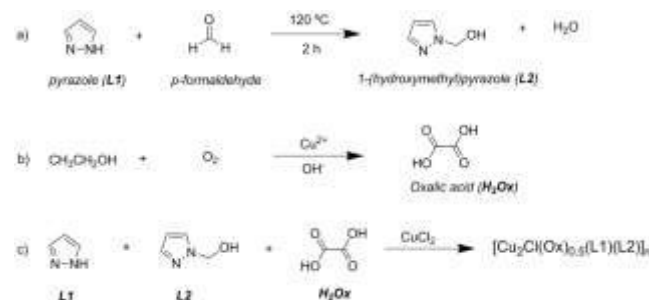
The unexpected formation of the oxalate anion in the reaction medium could be attributed to the ethanol oxidation by the dissolved O₂, favored by the basicity of the medium and the

Table 2. Crystallographic data for copper(II) complex.

Molecular Formula	$\text{C}_8\text{H}_8\text{ClCu}_2\text{N}_4\text{O}_3$
Formula weight	370.71
Temperature (K)	100(2)
Wavelength (Å)	0.71073
System, space group	Monoclinic, P 2 ₁ /c
Unit cell dimensions	
a (Å)	10.5078 (7)
b (Å)	9.1266 (6)
c (Å)	11.7875 (8)
α (°)	90
β (°)	99.869 (3)
γ (°)	90
U (Å ³)	1113.70 (13)
Z	4
D _{calc} (mg m ⁻³)	2.211
μ (mm ⁻¹)	4.062
F(000)	732
Crystal size (mm ³)	0.290x0.252x0.145
hkl ranges	-13 ≤ h ≤ 13 -11 ≤ k ≤ 11 -14 ≤ l ≤ 14
2 θ Range (°)	2.84 to 26.37
Reflections collected/unique/ [R _{int}]	13166/2283 [R(int) = 0.0344]
Completeness to θ	99.8% (θ = 25.242°)
Absorption correction	Semi-empirical from equivalents
Data/restraints/parameters	2283/54/163
Goodness-of-fit on F ²	1.058
Final R indices [I > 2 σ (I)]	R1 = 0.0208, wR ₂ = 0.0545
R indices (all data)	R1 = 0.0232, wR ₂ = 0.0559
Largest diff. peak and hole (e Å ⁻³)	0.444 and -0.412

catalytic properties of the copper(II) ions (the reaction took place in aerobic and basic conditions). Copper(II) ions could produce the catalytic activation of O₂ and OH⁻ to produce reactive species (i.e. hydroxyl radicals, OH[•]) being capable of oxidizing a minor fraction of ethanol solvent. By spectrophotometric method traces of oxalic acid were found after stirring a basic solution of ethanol and CuCl₂ under aerobic condition.²⁷ Similar oxalate sensing was reported by Jing Su *et al.*²⁸ and Mansour Arab *et al.*²⁹ The possible reactions involved in the synthesis process of the complex here-presented are illustrated in **Scheme 1**.

The “*in situ*” formation of oxalic acid from solvent during the complex formation reaction has been previously reported.^{30,31} In addition, there are also previous reports of the aerobic alcohol oxidation during the formation of copper coordination complexes or in the presence of copper salts.^{32–34} In all these cases the alcohol oxidation is related to the catalytic properties of copper(II) ions.



Scheme 1. Chemical reactions involved in the obtaining of the polymeric complex: synthesis of the L2 ligand (a), *in situ* formation of oxalic acid (b) and complex formation (c).

Copper, with dynamic Jahn-Teller distortion,³⁵ catalyzes efficiently the oxidation of organic compounds under mild conditions and can provide open Lewis acid sites which are effective for catalysis of various organic reactions such as azide-alkyne cycloaddition, oxidative coupling reaction, Henry reaction or Diels-Alder reaction,³⁶⁻³⁸ or water oxidation³⁹ among others. This binuclear copper(II) based coordination polymer owes the particularity that it is composed of three different ligands, where none of [CuClO₃N_{pz}] and [N_{pz}-Cu-Ox-Cu-N_{pz}] coordination environment have been reported before.⁴⁰ Only the [CuClO(N_{pz})₂] core presents similar coordination spheres already described.²⁰⁻²³ Such special coordination spheres provide interesting structures to the network of this complex.

At the supramolecular crystal arrangement, each [Cu₄Cl₂(Ox)(L1)₂(L2)₂] molecule is surrounded by other 4 neighbouring molecules in the unit cell. The disposition of these molecules in the unit cell is a typical ABAB structure. Zig-zag layers of polymeric chains interconnected by chloride bridges between the intermolecular copper centers afford a 2D structure along the *b* axis at the supramolecular framework (Figure 2A). The chlorine atoms (Cl1) are the bridges between one molecule and other through the Cu2-Cl1-Cu1 bond with 93.02° angle. In addition, the intramolecular contacts between the N3...Cl1...N2 atoms (3.086 and 3.111 Å, respectively) contribute to support the supramolecular network (Figure 2B). The layered structure staggered determines the mechanical properties measured in this polymer by the nanoindentation technique.

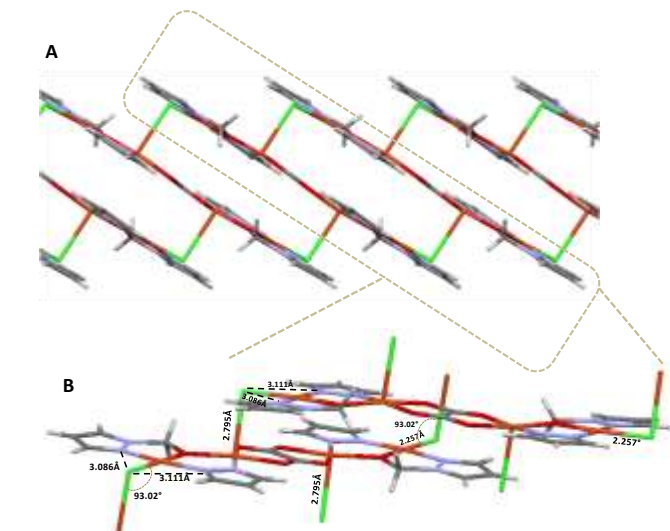


Figure 2. A) Polymeric layer structure with zig-zag distribution along the *b* axis. B) The close-up view displays the distances and the angles formed by the Cu1-Cl1-Cu2 intermolecular bridges.

3.2 Mechanical properties of the binuclear copper(II) based coordination polymer

Representative nanoindentation curves, performed perpendicular to the 2D crystal sheet, and up to maximum loads of 1.2 and 2.8 mN are shown in Fig. 3a and Fig. S1. Measurement of the mechanical properties by nanoindentation along other directions was not possible because of the high tendency for the crystals towards brittle fracture. Discontinuities or pop-in events in the loading segments are often observed and are ascribed to the breakage of molecular stacks and the concomitant sudden penetration of the indenter deeper into the sample. Atomic force microscopy images (Fig. 3b) of an indentation performed using a maximum load of 2.8 mN shows that pile-up

effects are virtually not present, while crack formation from the edge of the triangular imprint is sometimes formed, an observation which is in agreement with the occurrence of serrations in the loading segments of the indentation curves (Fig. 3a). The lack of pile-up avoids artifacts related to the determination of the contact area from the contact depth, when using the method of Oliver and Pharr.¹⁶

The values of hardness, reduced Young's modulus, indentation energies and elastic recovery (W_{el}/W_{tot}) are shown in Fig. 4(a) and Fig. 4(b), respectively. Hardness remains rather constant ($H \approx 0.4-0.5$ GPa) as a function of the applied maximum load (Fig. 4a). This value is a bit higher than the ones reported by C. M. Reddy *et al.*⁴¹ for 2-(methylthio)nicotinic acid and similar to values reported by J. C. Tan *et al.* in different low-symmetry polymorphs of copper phosphonacetates [Cu_{1.5}(H₂O)(O₃PCH₂CO₂)].⁴² Conversely, the Young's modulus is a bit lower than the values reported in some other molecular crystals^{13,42,43} but similar to the values reported by A. Samanta *et al.* in [OZn₄(BDC)₃]_n, where BDC stands for 1,4-benzenedicarboxylate anion.⁴⁴ The increase of E_r with the applied load indicates a higher resistance against elastic deformation as the penetration depth is progressively increased. This could be due to the larger amount of molecular bonds which hinder the elastic deformation as the applied load is progressively increased. Nevertheless, no clear changes in the elastic energy or the elastic recovery are observed in the range of applied loads used in this study (Fig. 4b). The values of elastic recovery ($W_{el}/W_{tot} \approx 0.6$) are clearly larger than those in other types of organic-inorganic materials⁴⁵ and comparable to the values in some recent reports on 3D inorganic composite films.⁴⁶

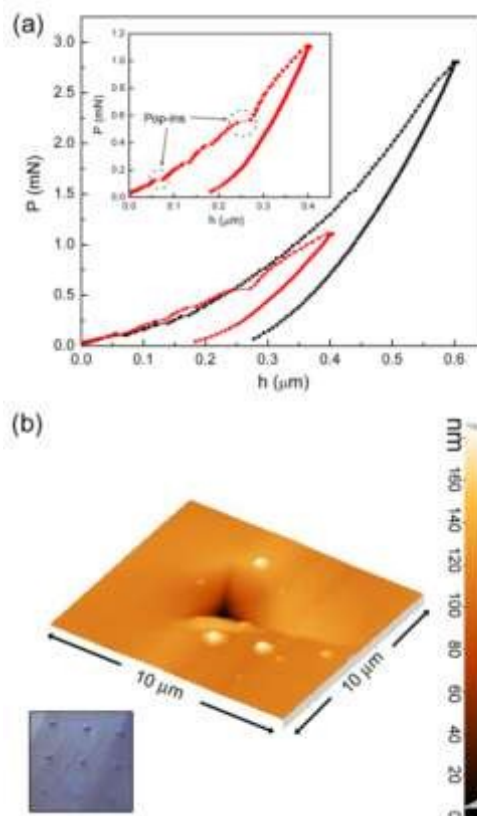


Figure 3. a) Representative nanoindentation curves performed perpendicular to the crystal sheet, and up to maximum loads of 1.2 mN (red line) and 2.8 mN (black line). b) Atomic force microscopy and optical (inset) images of an indentation performed using a maximum load of 2.8 mN.

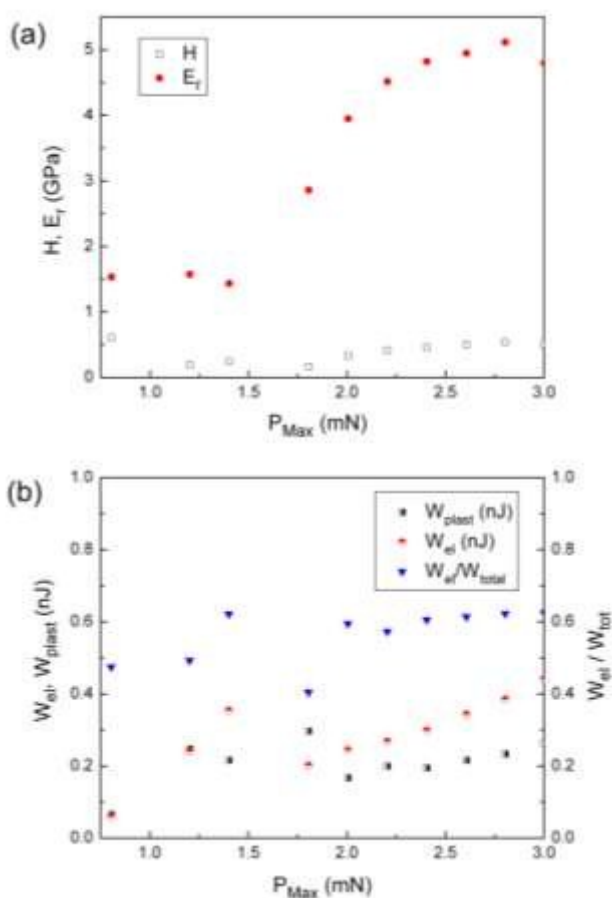


Figure 4. Values of a) Hardness, Reduced Young's Modulus and b) indentation energies and elastic recovery (W_{el}/W_{tot}) of the complex.

4. Conclusions

A new binuclear copper(II) complex with polymeric structure has been unexpectedly obtained from a mixture of pyrazolic ligands and CuCl_2 in ethanol medium. The two copper(II) centers have different coordination numbers and geometries. The Cu1 atom is four-coordinated in the $[\text{CuClO}(\text{N}_{pz})_2]$ core with square-planar molecular geometry, while the Cu2 nucleus is five-coordinated with $[\text{CuClO}_3\text{N}_{pz}]$ core and exhibits square-pyramidal geometry. Furthermore, the Cu2 centers of different molecular units are interconnected in the polymeric structure by one unexpected oxalate anion. The terminal chlorine atoms act as bridges between the monomeric units in this coordination polymer. As far as we know, it is the first time that the $[\text{CuClO}_3\text{N}_{pz}]$ and the $[\text{N}_{pz}\text{-Cu-Ox-Cu-N}_{pz}]$ coordination environments are reported. At supramolecular network an interesting 2D structure with layered architecture formed by polymeric chains interconnected by Cu2-Cl1-Cu1 bridges affords through the b -axis. Additionally, the values of hardness, Young's modulus, and elastic recovery of this structure have been determined by means of nanoindentation. The mechanical characterization of this kind of hybrid materials is an important asset on crystal engineering since durability and reliability, which are dictated by the mechanical properties, are important factors for their potential applications in sensors, catalysts and gas storage, among others.

Acknowledgements

The financial support from the MAT2011-27380-C02-01 and the MAT2011-27225 research projects from the Spanish MINECO, and the 2014-SGR-1015 and the 2014-SGR-260 projects from the Generalitat de Catalunya is acknowledged. M. D. B. was partially supported by an ICREA-Academia award. A. L. M. thanks the FI-2010 scholarship given by the Government of Catalonia. M. G. acknowledges the support of the Secretary for Universities and Research of the Government of Catalonia and the COFUND Programme of the Marie Curie Actions of the 7th R&D Framework Programme of the European Union for the 'Beatriu de Pinos' contract (2013 BP-B 00077). E. P. acknowledges the Spanish MINECO for the 'Ramon y Cajal' contract (RYC-2012-10839).

Notes and references

- ^a Departament de Química, Universitat Autònoma de Barcelona, E-08193 Bellaterra, Spain
^b Departament de Física, Universitat Autònoma de Barcelona, E-08193 Bellaterra, Spain.
^c Cristal·lografia, Mineralogia i Dipòsits Minerals, Universitat de Barcelona, 08028-Barcelona, Spain
^d Unitat de Difracció de RX. Centres Científics i Tecnològics de la Universitat de Barcelona (CCiTUB). Universitat de Barcelona.08028-Barcelona
^e Institució Catalana de Recerca i Estudis Avançats (ICREA), Departament de Física, Universitat Autònoma de Barcelona, E-08193 Bellaterra, Spain. *Corresponding authors' contacts: Miguel.Guerrero@uab.cat, Phone: +34 93 581 1401

[†]These authors have equally contributed to this work.

§The X-ray crystallographic file in CIF format for the structure determination of the polymeric Cu(II) complex is enclosed. This information is available free of charge via the internet at <http://pubs.acs.org>. The CCDC 1036962 contains the supplementary crystallographic data for this complex. This data can be obtained free of charge via: <http://www.ccdc.cam.ac.uk/conts/retrieving.html> or from the Cambridge Crystallographic Data Centre, 12 Union Road, Cambridge CB2 1EZ, UK; fax: (+44) 1223-336-033; or email: deposit@ccdc.cam.ac.uk.

References

- T. R. Cook, Y.-R. Zheng and P. J. Stang, *Chem. Rev.*, 2013, **113**, 734-777.
- M. Eddaoudi, J. Kim, N. Rosi, D. Vodak, J. Wachter, M. O'Keeffe and O. M. Yaghi, *Science*, 2002, **295**, 469-472.
- I.-H. Park, A. Chanthapally, Z. Zhang, S. S. Lee, M. J. Zaworotko and J. J. Vittal, *Angew. Chem., Int. Ed.*, 2014, **53**, 414-419.
- S. Xiang, Y. He, Z. Zhang, H. Wu, W. Zhou, R. Krishna and B. Chen, *Nat. Commun.* 2012, **3**, 954-963.
- X.-L. Yang, M.-H. Xie, C. Zou, Y. He, B. Chen, M. O'Keeffe and C.-D. Wu, *J. Am. Chem. Soc.* 2012, **134**, 10638-10645.
- Y. Zhao, D.-S. Deng, L.-F. Ma, B.-M. Ji and L.-Y. Wang, *Chem. Commun.*, 2013, **49**, 10299-10301.
- L. Croitor, E. B. Coropceanu, D. Chisca, S. G. Baca, J. van Leusen, P. Kögerler, P. Bourrosh, V. Ch. Kravtsov, D. Grabco, C. Pyrtsac and M. S. Fonari, *Cryst. Growth Des.*, 2014, **14**, 3015-3025.
- L. J. McCormick, S. G. Duyker, A. W. Thornton, C. S. Hawes, M. R. Hill, V. K. Peterson, S. R. Batten and D. R. Turner, *Chem. Mater.*, 2014, **26**, 4640-4646.
- F. Gul-E-Noor, M. Mendt, D. Michel, A. Pöppel, H. Krautscheid, J. Haase and M. Bertmer, *J. Phys. Chem. C*, 2013, **117**, 7703-7712.
- J. Ch. Tan and A. K. Cheetham, *Chem. Soc. Rev.*, 2011, **40**, 1059-1080.
- W. Li, M. S. R. N. Kiran, J. L. Manson, J. A. Schlueter, A. Thirumurugan, U. Ramamurthy and A. K. Cheetham, *Chem. Commun.*, 2013, **49**, 4471-4473.
- S. Varughese, M. S. R. N. Kiran, U. Ramamurthy and G. R. Desiraju, *Angew. Chem., Int. Ed.*, 2013, **52**, 2701-2712.

- ¹³ J. C. Tan, J. D. Furman and A. K. Cheetham, *J. Am. Chem. Soc.*, 2009, **131**, 14252-14254.
- ¹⁴ S. S. Han and W. A. Goddard, *J. Phys. Chem. C*, 2007, **111**, 15185-15191.
- ¹⁵ W. L. Driessen, *Recul. Trav. Pais-Bas*, 1982, **101**, 441-443.
- ¹⁶ W. C. Oliver, and G. M. Pharr, *J. Mater. Res.*, 1992, **7**, 1564-1583.
- ¹⁷ A. Fischer-Cripps, *Nanoindentation*, Springer, New York, USA, 2004.
- ¹⁸ E. Pellicer, A. Varea, S. Pané, B. J. Nelson, E. Menéndez, M. Estrader, S. Suriñach, M. D. Baró, J. Nogués and J. Sort, *Adv. Funct. Mater.*, 2010, **20**, 983-991.
- ¹⁹ Analysis for $C_8H_8ClCu_2N_4O_3$ calcd/found (%): C, 25.92/25.72; H, 2.17/2.13; N, 15.11/15.04; Cu, 34.28/33.96 giving a satisfactory C, H, N and Cu elemental analyses. IR(KBr, cm^{-1}): 3190, 3120 $\nu(C-H)_{ar}$; 2940, 2920 $\nu(C-H)_{al}$; 1650 $[\nu(C=C)]_{ar}$; 1400 $[\delta(C=C)]_{ar}$, $\delta(C=N)_{ar}$ and 773 $\gamma(C-H)_{oop}$ present shifts (in relation with the free ligand) produced by the coordination with copper(II), moreover the bands at 472, 428 $\nu(Cu-N)$; 550, $\nu(Cu-O)$; 600 $\gamma_{as}(Cu-O)$ and 356, 322 $\nu(Cu-Cl)$ corroborate the copper coordination too. Conductivity (1.02×10^{-3} M in methanol): $32 \Omega^{-1}cm^2mol^{-1}$ in agreement with a non-electrolyte complex. UV-vis (1.1×10^{-3} M in methanol) exhibits a single band at 620 nm.
- ²⁰ G. Mezei, M. Rivera-Carrillo and R. G. Raptis, *Inorg. Chim. Acta*, 2004, **357**, 3721-3732.
- ²¹ G. Mezei, R. G. Raptis and J. Telsler, *Inorg. Chem.*, 2006, **45**, 8841-8843.
- ²² M. Rivera-Carrillo, I. Chakraborty, G. Mezei, R. D. Webster and R. G. Raptis, *Inorg. Chem.*, 2008, **47**, 7644-7650.
- ²³ P. A. Angaridis, P. Baran, R. Boca, F. Cervantes-Lee, W. Haase, G. Mezei, R. G. Raptis and R. Werner, *Inorg. Chem.*, 2002, **41**, 2219-2228.
- ²⁴ M. F. Castello, C. V. Grupioni, R. S. Nunes and J. M. Luiz, *J. Therm. Anal. Calorim.*, 2014, **117**, 1145-1150.
- ²⁵ X.-D. Zhang, Z. Zhao, J.-Y. Sun, Y.-Ch. Ma and M.-L. Zhu, *Acta Crystallogr., Sect. E.*, 2005, **61**, m2643-m2645.
- ²⁶ H.-D. Wang, Y.-L. Zhou, H.-Y. He, X.-H. Tu and L.-G. Zhu., *Acta Crystallogr., Sect. E.*, 2006, **62**, m1081-m1082.
- ²⁷ Traces of oxalic acid were determined by spectrophotometric method under aerobic conditions after stirring a basic solution of $CuCl_2$ in ethanol. The oxalic acid concentration was determined by the decrease in absorbance of the Cu^{2+} band and the increase of the Cu-Ox one changing the colour from blue to yellow.
- ²⁸ J. Su, Y.-Q. Sun, F.-J. Huo, Y.-T. Yang and C.-X. Yin, *Analyst*, 2010, **135**, 2918-2923.
- ²⁹ M. Arab Chamjangali, L. Sharif-Razavian, M. Yousefi and A. Hossein Amin, *Spectrochimica Acta Part A*, 2009, **73**, 112-116.
- ³⁰ O. R. Evans and W. Lin, *Cryst. Growth Des.*, 2001, **1**, 9-11.
- ³¹ Ch. S. Hawes and P. E. Kruger, *Aust. J. Chem.*, 2013, **66**, 401-408.
- ³² I. Gamba, I. Mutikainen, E. Bouwman, J. Reedijk, and S. Bonnet, *Eur. J. Inorg. Chem.* **2013**, 115-123.
- ³³ N. Mase, T. Mizumori, Y. Tatemoto, *Chem. Commun.*, 2011 **47**, 2086-2088.
- ³⁴ R. A. Sheldon, *Catal. Today*, 2014, doi:10.1016/j.cattod.2014.08.024.
- ³⁵ M. A. Halcrow, *Chem. Soc. Rev.*, 2013, **42**, 1784-1795.
- ³⁶ J. Park, J.-R. Li, Y.-P. Chen, J. Yu, A. A. Yakovenko, Z. U. Wang, L.-B. Sun, P. B. Balbuena and H.-C. Zhou, *Chem. Commun.*, 2012, **48**, 9995-9997.
- ³⁷ I. H. Hwang, J. M. Bae, W.-S. Kim, Y. D. Jo, Ch. Kim, Y. Kim, S.-J. Kim and S. Huh, *Dalton Trans.*, 2012, **41**, 12759-12765.
- ³⁸ Y. Zhao, D.-Sh. Deng, L.-F. Ma, B.-M. Ji and L.-Y. Wang, *Chem. Commun.*, 2013, **49**, 10299-10301.
- ³⁹ Teng Zhang, Cheng Wang, Shubin Liu, Jin-Liang Wang, and Wenbin Lin, *J. Am. Chem. Soc.* 2014, **136**, 273-281.
- ⁴⁰ Cambridge Crystallographic Data Centre, 12 Union Road, Cambridge CB2 1EZ, UK.
- ⁴¹ C. M. Reddy, R. C. Gundakaram, S. Basavoju, M. T. Kirchner, K. A. Padmanabhan and G. R. Desiraju, *Chem. Commun.*, 2005, 3945-3947.
- ⁴² J. C. Tan, C. A. Merrill, J. B. Orton and A. K. Cheetham, *Acta Materialia*, 2009, **57**, 3481-3496.
- ⁴³ C. Malla, G. Reddy, R. Krishnaa and S. Ghosha, *CrystEngComm*, 2010, **12**, 2296-2314.
- ⁴⁴ A. Samanta, T. Furuta and J. Li, *J. Chem. Phys.*, 2006, **125**, 084714/1-084714/8.
- ⁴⁵ C. Schütz, J. Sort, Z. Bacsik, V. Oliynyk, E. Pellicer, A. Fall, L. Wågberg, L. Berglund, L. Bergström and G. Salazar-Álvarez, *PlosOne*, 2012, **7**, e45828.
- ⁴⁶ M. Guerrero, S. Pané, B. J. Nelson, M. D. Baró, M. Roldán, J. Sort, and E. Pellicer, *Nanoscale*, 2013, **5**, 12542-12550.